Earth Science Informatics (2024) 17:21–35
https://doi.org/10.1007/s12145-023-01148-8

RESEARCH

Assessing the quality of raw GNSS observations and 3D positioning performance using the Xiaomi Mi 8 dual-frequency smartphone in Northwest Mexico

J. Rene Vazquez-Ontiveros[1] · Carlos A. Martinez-Felix[2] · Angela Melgarejo-Morales[3] · Leire Retegui-Schiettekatte[4] · G. Esteban Vazquez-Becerra[1] · J. Ramon Gaxiola-Camacho[5]

Received: 16 August 2023 / Accepted: 6 November 2023 / Published online: 22 November 2023

Abstract

GNSS observations from smartphones have gained popularity in recent years due to the high precision achieved in various applications. While most studies have focused on signal quality evaluation, few have explored static and kinematic positioning. Furthermore, the majority of these studies have primarily concentrated on European and Asian countries. Therefore, we present the first study conducted in Northwest Mexico, which evaluates the performance of static and kinematic positioning using code and phase observations obtained from the Xiaomi Mi 8 smartphone. In addition, we assess the signal quality of ~ 100 available GNSS satellites. This study proposes an alternative method for analyzing the observed Carrier-to-Noise Density Ratio (C/N_0) of GNSS observations in relation to theoretical reference values. The results reveal that the average C/N_0 value of the GNSS satellites is approximately 18% lower than the reference values. Furthermore, the pseudorange observations indicate a significant multipath error, with magnitudes close to 200 cm for L1/E1 and less than 86 cm for L5/E5a, highlighting the susceptibility of the smartphones GNSS antenna to this type of error. The static experiment demonstrates RMS positioning errors of 0.7 cm, 1.2 cm, and 4.2 cm for the E, N, and U components, respectively. Moreover, the kinematic experiment exhibits discrepancies of 1.4 cm due to the circular trajectory of the smartphone. Finally, the results suggest that dual-frequency smartphones offer promising positioning capabilities, presenting opportunities for engineering applications, including structural health monitoring, among others.

Keywords Smartphone Xiaomi Mi 8 · Kinematic and static positioning · Quality analysis · Multipath · Carrier-to-noise density ratio · GNSS

Communicated by: H. Babaie

✉ Carlos A. Martinez-Felix
carlosmartinez@uas.edu.mx

J. Rene Vazquez-Ontiveros
jesusrene@uas.edu.mx

Angela Melgarejo-Morales
angela@igeofisica.unam.mx

Leire Retegui-Schiettekatte
leirears@plan.aau.dk

G. Esteban Vazquez-Becerra
gvazquez@uas.edu.mx

J. Ramon Gaxiola-Camacho
jrgaxiola@uas.edu.mx

[1] Department of Earth and Space Sciences, Autonomous University of Sinaloa, Culiacan, Sinaloa, Mexico

[2] Department of Physics-Mathematics Science, Autonomous University of Sinaloa, Culiacan, Sinaloa, Mexico

[3] SCiESMEX, LANCE, Instituto de Geofísica, Unidad Michoacán, Universidad Nacional Autónoma de México, Michoacan C.P. 58089, Morelia, México

[4] Geodesy Group, Department of Planning and Sustainability, Aalborg University, Rendsburggade 14, Aalborg 9000, Denmark

[5] Department of Civil Engineering, Autonomous University of Sinaloa, Culiacan, Sinaloa, Mexico

Introduction

Smartphones and tablets have become essential electronic devices in the daily lives of many people, offering a wide range of services and applications that simplify various everyday tasks and operations. Among these basic services, navigation applications stand out, relying on GNSS positioning technology for accurate location information. In the past, smartphones faced technical limitations in positioning, leading to reduced accuracy and performance due to limited access to pseudorange, Doppler, or carrier-phase observables (Robustelli et al. 2019; Chen et al. 2019; Geng and Li 2019). Since the release of Android operating system version 7.0 in 2016, raw GNSS measurements have become accessible for compatible devices, providing an opportunity for the GNSS research community to assess and enhance timing, positioning, and navigation applications using smartphones (Li and Geng 2019; Paziewski 2020; Dabove et al. 2020; Liu et al. 2021). The built-in chipsets have also advanced significantly, allowing the evaluation of positioning capabilities in various modalities, such as RTK (Real-time Kinematic) (Odolinski and Teunissen 2019; Gao et al. 2021; Yong et al. 2021, 2022), single and dual-frequency PPP (Precise Point Positioning) (Liu et al. 2019; Wu et al. 2019; Wen et al. 2020; Wang et al. 2021; Yi et al. 2021, 2022; Shinghal and Bisnath 2021; Li et al. 2021) and relative positioning (Paziewski et al. 2019, 2021).

In recent years, built-in smartphone chipsets have undergone significant advancements. Between 2016 and 2018, many chipsets were multi-constellation but single-frequency, requiring the use of models like Klobuchars to estimate ionospheric error, which resulted in performance limitations. A breakthrough occurred in 2018 with the release of the Xiaomi Mi8, the first dual-frequency GNSS smartphone featuring the Broadcom BCM47755 chipset. This cutting-edge chip can track GPS (L1, C/A, L5), GLONASS (G1), BeiDou (B1), QZSS (L1, L2), and Galileo (E1, E5a) (Guo et al. 2020). However, it should be noted that the Samsung S23 series, equipped with the same chipset, only records code observations, failing to fully utilize the dual-frequency capabilities. The accuracy of the raw GNSS measurements from the Xiaomi Mi8 and Mi9 models was assessed in the studies conducted by Chen et al. 2019 and Robustelli et al. 2021. These studies assumed that the duty cycle had no influence on the operator phase and that the L5/E5 frequency observations exhibited higher quality compared to the L1/E1 frequency data. In the literature, several studies focusing on the performance of smartphones in differential or relative positioning approaches are available. For example, Bahadur (2022) conducted a kinematic experiment using three smartphones in a real-time standalone positioning scenario. By utilizing single-frequency code observations, the study revealed an average improvement of 11% in the positioning accuracy of the smartphones. Similarly, Aggrey et al. (2020) explored the potential of enhancing positioning accuracy through raw GNSS data obtained from dual-frequency chipsets. The results demonstrated notable improvements in both static and kinematic positioning over a 6-hour period, especially during the initial minutes. Furthermore, Bakuła et al. (2020, 2022), evaluated the performance of pseudorange measurements in smartphone positioning, comparing the L1 and L5 frequencies using Differential Global Position System (DGPS) and Differential Global Navigation Satellite System (DGNSS). The findings indicated that using the L5 code, a centimeter-level accuracy in 3D positioning can be achieved, with the capability to track 16 to 26 satellites. Additionally, Fortunato et al. (2019) conducted a study utilizing a Xiaomi Mi8 to evaluate the devices positioning capabilities for geophysical applications, including real-time observations and ionosphere monitoring. The research revealed that in a static scenario, the noise level for the horizontal and vertical position components was in the order of millimeters and centimeters, respectively. The experimental results demonstrated that the Standalone Positioning (SPP) approach could obtain similar results to the Differential Global Navigation Satellite System (DGNSS) solution, achieving positioning accuracy typically in the order of meters. Another study by Pepe et al. (2021) established that DGNSS generally outperforms SPP for altimetric positioning. Similarly, Realini et al. (2017) examined the accuracy and feasibility of relative positioning using a single-frequency smartphone in relation to a base station. The research revealed that decimeter-level accuracy can be achieved with raw GNSS phase observations without phase ambiguity resolution. More recent studies have focused on analyzing the positioning accuracy of low-cost smartphones in different environments, such as urban areas (Specht et al. 2020; Uradziński and Bakuła 2020) and forests (Tomaštík et al. 2021; Tomaštík and Varga 2021). These experiments concluded that GNSS adverse effects, particularly multipath, significantly degrade the quality and accuracy of smartphone positioning (Zhu et al. 2020). However, when compared to single-frequency smartphones, multi-constellation dual-frequency devices offered more reliable and accurate position measurements (Wanninger and Heßelbarth 2020; Zangenehnejad and Gao 2021; Yong et al. 2022). Moreover, it was assessed the GNSS performance capabilities using low-end hardware in Android smartphones, since most studies are based on high-end hardware which implies better internal components. The results demonstrate that the observable data quality of these smartphones maintain low performance

compared to flagships smartphones (Bramanto et al. 2023). Furthermore, other research work conducted by Li et al. (2023) evaluate the high-precision velocity using GNSS measurements retrieved by Android smartphones using the App Geo++RINEX Logger. The authors stated that the Doppler-estimated receiver clock drifts in conjunction with frequent jumps leads to anomalous clock variations. Finally, Cheng et al. (2023) proposed an alternative approach for real-time kinematic precise point positioning (PPP-RTK) using GNSS data recorded by Android smartphones. The results indicated that the post-processing time needed to achieve centimeter-level precisions in stand-alone mode is ~ 1 min, which provide a relatively rapid approach for high-precision GNSS positioning using smartphones.

In conclusion, there is a growing interest in utilizing low-cost smartphones with integrated GNSS chipsets for positioning applications, and numerous studies are being conducted to evaluate their positioning accuracy. It is essential to assess the quality and performance of these devices in various regions worldwide, including mid-latitudes, as highlighted in studies by Zhang et al. (2018) and Zeng et al. (2022). Such evaluations will be crucial for advancing these smartphones into professional-level surveying devices in the near future.

Considering all the aspects discussed above, the aim of this study is to analyze the signal quality for each satellite observed using a newly proposed method that incorporates theoretical observations of the Carrier-to-Noise Density Ratio (C/N_0). We evaluated the performance of kinematic and static positioning using raw observations a Xiaomi Mi 8 smartphone equipped with a dual-frequency Broadcom BCM47755 chipset in Northwest Mexico. Quality analysis involves examining GNSS signals over a 24-hours measurement period, focusing on the visibility of individual satellite, constellations, and frequencies. Furthermore, the performance of kinematic positioning is evaluated considering tracking a circular trajectory. The paper is organized as follows: Section "Experimental setup and data acquisition" describes the experimental setup and data acquisition, encompassing static and kinematic measurements. Section "Static GNSS measurements" provides a description of the different parameters utilized to assess GNSS signal quality. Section "Kinematic GNSS measurements" presents the analysis and experimental findings of this study. In Sections. "GNSS signal quality assessment" and "Carrier-to-noise density ratio (C/N0)", the results and conclusions are discussed.

Experimental setup and data acquisition

GNSS observations from a Xiaomi Mi 8 smartphone were collected and evaluated under three different settings: static positioning for signal quality assessment over a long period, dynamic positioning performance evaluation, and three-dimensional positioning in a static test. Detailed methodologies for each setting will be presented in subsequent sections.

The Xiaomi Mi 8 smartphone is equipped with the Broadcom BCM47755 dual GNSS chip, capable of receiving simultaneous signals as listed in Table 1. In the Table, the observables correspond to the RINEX 3.04 format recorded by the smartphone using the Geo++Rinex Logger APP. Unlike other smartphone models, the Xiaomi Mi 8 possesses the advantage of acquiring both code and phase observables from all GNSS constellations, with the duty cycle disabled.

Static GNSS measurements

The Xiaomi Mi 8 smartphone was vertically positioned with support on a forced centering monument on the roof of a residential house, as shown in Fig. 1. The concrete monuments location provided good signal coverage and optimal measurement conditions, with minimal possibilities of generating multipath due to the absence of obstructions. Any multipath values obtained were predominantly attributed to the smartphones embedded antenna characteristics. In the first experiment, the objective was solely to evaluate the acquired GNSS signal, eliminating the need for conventional centering. Additionally, maintaining a static position

Table 1 GNSS signals that the Xiaomi Mi 8 smartphone can track. C represents the code observation, L is the phase observable, D is the Doppler measurement, S is the noise measurement, G denotes the GPS constellation, R stands for GLONASS, E for Galileo, C for BeiDou, and J for QZSS

Smartphone	Chipset	Duty cycle	GNSS system	# of observable	Observables
Xiaomi Mi 8	Broadcom BCM47755	NO	G	8	C1C, L1C, D1C, S1C, C5X, L5X, D5X ,S5X
			R	4	C1C, L1C, D1C, S1C
			E	8	C1C, L1C, D1C, S1C, C5X, L5X, D5X, S5X
			C	4	C2I, L2I, D2I, S2I
			J	8	C1C, L1C, D1C, S1C, C5X, L5X, D5X, S5X

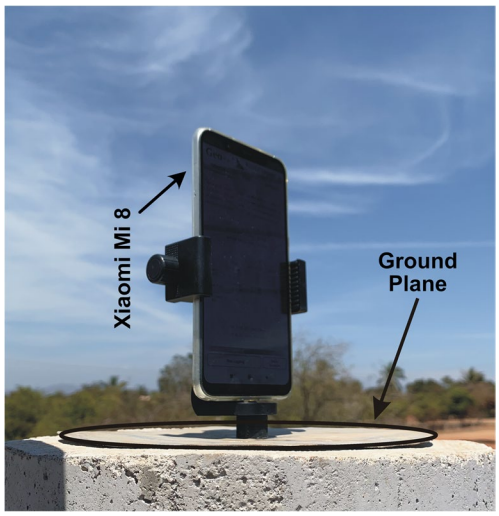

Fig. 1 Xiaomi Mi 8 smartphone on the concrete monument during GNSS measurements. A ground plane was positioned underneath the smartphone to mitigate multipath effects

ensured that changes in the antennas position would not affect the behavior of the quality parameters. C/N_0 and multipath were chosen as quality parameters, as they are commonly used to evaluate GNSS signals from smartphones (Robustelli et al. 2019; Paziewski et al. 2019, 2021; Guo et al. 2020; Wanninger and Heßelbarth 2020).

On 15th January 2023, 24-hour continuous raw GNSS observations were collected from the Xiaomi Mi 8 smartphone at a sampling rate of 1 Hz, with an elevation mask set at 0 degrees. The low elevation mask ensured tracking of all GNSS satellites, enabling correlation with the quality parameters evaluated in this study. For the static experiments measurement period, Bluetooth and Wi-Fi functions were disabled, and the Geo++Rinex Logger app was used to store the measurements in RINEX 3.04 format. The "Force Full GNSS Measurements" native function was enabled to remove smartphone battery power-saving (duty cycle) during measurements. The Anubis software was used to extract the number of GNSS satellites per measurement epoch, as well as the values of the carrier/noise density ratio (C/N_0) and multipath for satellites with dual frequencies (Vaclavovic and Dousa 2015).

Figure 2 shows the skyplot and the number of GNSS satellites observed during the experiment, as well as the availability of bands for each satellite. Initially, difficulties were encountered in maintaining tracking of the Galileo and BeiDou satellites over extended measurement periods. However, this issue was resolved by resetting the parameters of the dual GNSS chip in the Xiaomi Mi 8 smartphone, resulting in significant improvements in the measurements of Galileo and BeiDou satellites, with only occasional and short-term track losses. Subsequently, it was identified that a regulation by the Federal Communications Commission (FCC) in the United States of America (USA) was causing the tracking issue with the Galileo and BeiDou constellations. The close proximity between the smartphone location and the USA led to potential interference with the Galileo and BeiDou signals. The FCC regulation stipulated that any non-federal receiver in the USA utilizing foreign GNSS signals must be licensed. Although the ban was later lifted by the FCC, many devices were not updated to track these constellations (FFC 2023). As a result, some nations currently have limited Galileo and BeiDou coverage on dual GNSS chips, depending on the smartphone manufacturer.

In Northwestern Mexico, a Xiaomi Mi 8 smartphone was able to acquire GNSS observations from 100 satellites, which consisted of 31 GPS satellites (12 dual-frequency L1, L5 and 19 single-frequency), 24 single-frequency GLONASS satellites (G1), 24 dual-frequency Galileo satellites (E1, E5a), and 21 single-frequency BeiDou satellites (B1). Among the BeiDou satellites, 3 were from the BDS-2 block, and 18 were from the BDS-3 block, with only the BeiDou Medium Earth Orbit (MEO) satellites being visible. The results obtained from the Xiaomi Mi 8 smartphone were consistent with the satellites tracked by the GNSS antenna HITAT35101CR HITS, a geodetic-order antenna from Hi Target located approximately 8 km away from the experimental area (See Fig. 2).

The number of satellites tracked for each constellation and frequency during all measurement times is shown in Fig. 3.

Kinematic GNSS measurements

The objective of this experiment was to assess the kinematic performance of the Xiaomi Mi 8 smartphone using multi-GNSS observations and considering different combinations (G, G+E, G+R+E+C, G+R+C). To achieve this, a circular motion device was designed, consisting of a servomotor capable of rotating at a speed of 0.44 rad/s and a 45 cm long metal bar centered over the axis of the servomotor. The Xiaomi Mi 8 smartphone was vertically positioned at a distance of 19 cm from the axis, as depicted in Fig. 4. During the kinematic experiment, observations were collected at 1 Hz with an elevation mask set at 10 degrees, covering signals from the GPS, GLONASS, Galileo, and BeiDou constellations. Additionally, given the known radius of the circular path, it is possible to determine, in each epoch, the distance between the center of rotation and the phase center of the smartphone. The measurement period extended approximately 5 h. Figure 5 illustrates the number of available satellites per constellation during the kinematic experiment.

The kinematic experiment was carried out under the same environmental conditions as the previous experiment. Post-processing was performed using the relative kinematic method with the RTKLIB software, utilizing the reference station equipped with the HITAT35101CR HITS antenna.

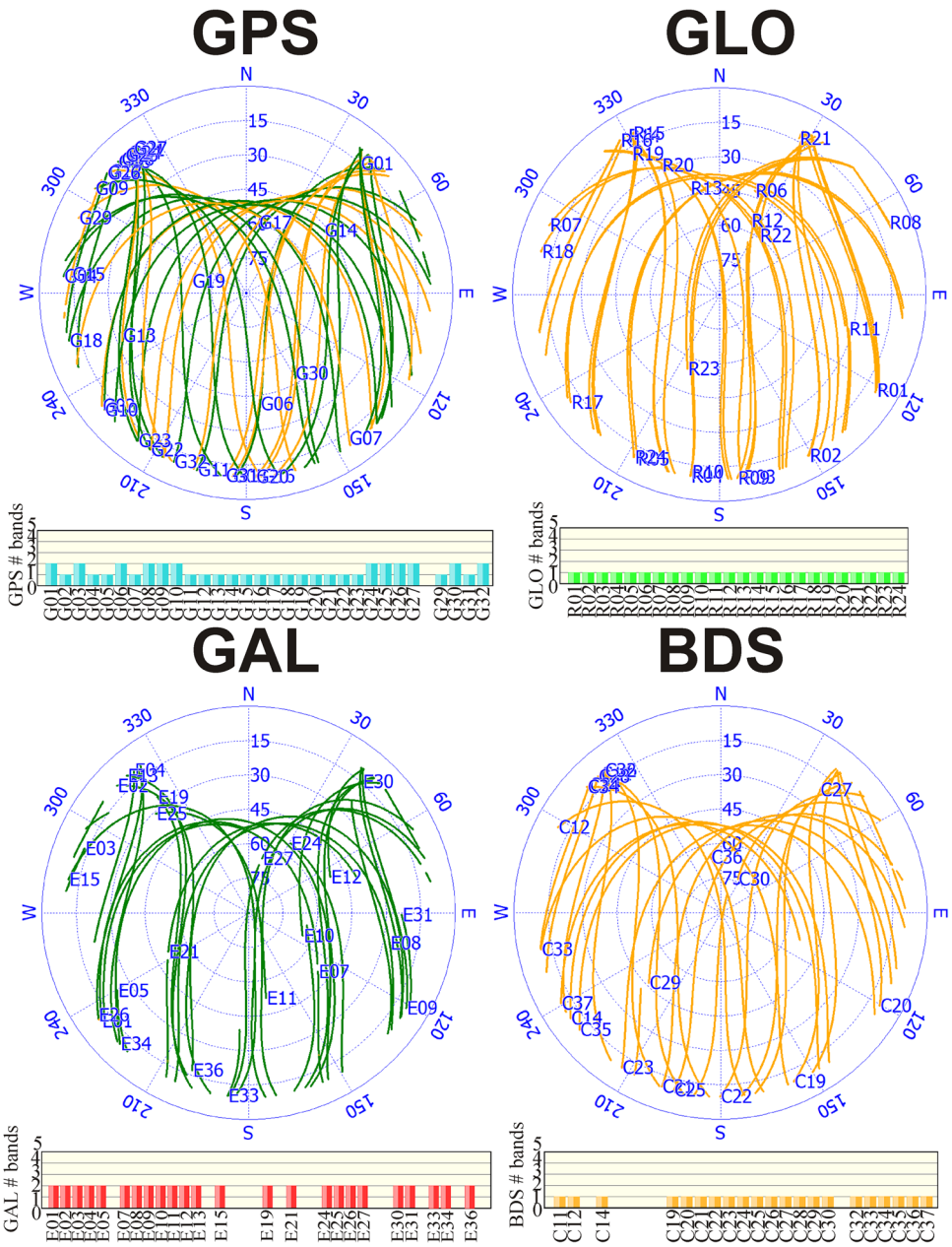

Fig. 2 Skyplot and number of available bands of the GNSS satellite tracked during the experiment in Northwest Mexico

GNSS signal quality assessment

This section evaluates the GNSS signal quality of the Xiaomi Mi 8 smartphone using two key indicators: The Carrier-to-Noise Density Ratio (C/N_0) and pseudorange multipath. Additionally, a novel approach is introduced to evaluate signal quality based on theoretical C/N_0 values for each frequency of the four global GNSS constellations.

Carrier-to-noise density ratio (C/N_0)

The strength of the GNSS signal is commonly measured using the Carrier-to-Noise Density Ratio (C/N_0) or Signal-to-Noise Ratio (SNR), which is indicative of the GNSS receivers' performance and the quality of carrier-phase and pseudorange observations. Geodetic antennas and receiver manufacturers analyze C/N_0 observations to improve their products technical specifications and signal quality acquisition. According to Langley (1997), the noise density (N_0) is affected by thermal noise sources, such as antenna and receiver temperature, which involve the motion of electrons within the receiver hardware. The noise temperature (T) for a typical receiver under normal conditions is approximately 290 K, leading to a noise density of -204 dBW/Hz when considering Boltzmann's constant $k = 1.38 \times 10^{-23} J/K$. On the other hand, the received carrier

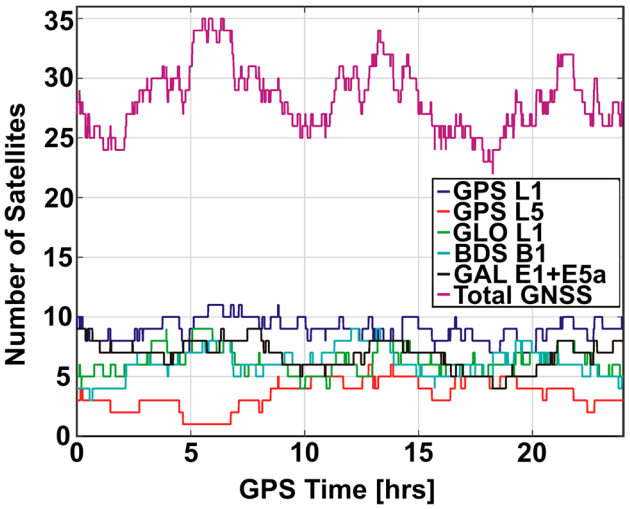

Fig. 3 Number of satellites tracked by GNSS constellation and frequency throughout the continuous 24-hour measurement period

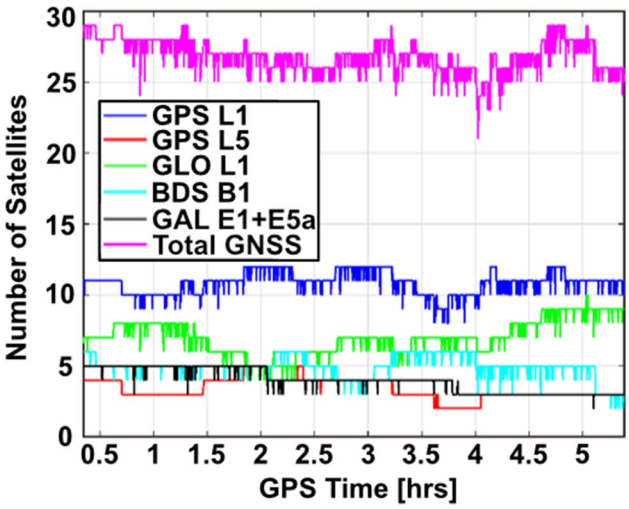

Fig. 5 Number of satellites available per GNSS constellation during the kinematic experiment

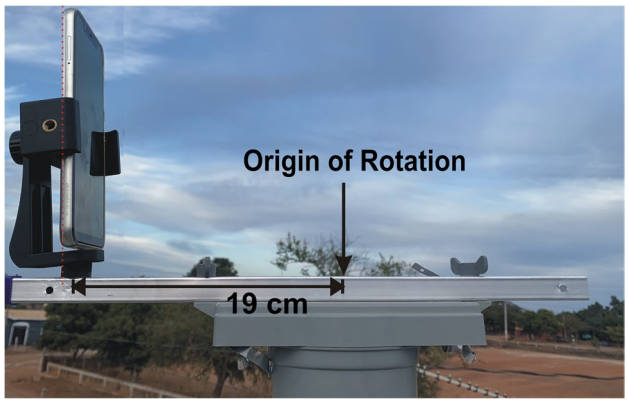

Fig. 4 The Xiaomi Mi 8 smartphone mounted on the rotary servo motor

power (C) is influenced by various factors, including satellite transmitter power output, changes in space loss, receiver antenna gain pattern, and signal losses between the antenna cable and receiver. For example, the nominal carrier power received for GPS L1 C/A is around − 158.5 dBW, representing the minimum signal level referenced to a 0 dB gain for an isotropic circularly polarized antenna. Additionally, the maximum received power (C_{MAX}) of a GNSS signal is crucial for calculating possible interference from the actual signal. Determining the maximum received power for a GNSS signal involves considering losses and gains of the signal propagation medium, incorporating spatial and physical factors such as: RF transmit power, equivalent transmit antenna gain towards the receiver antenna, gain of maximum received power with respect to the reference antenna, free space propagation loss at a given off-nadir angle, minimum possible atmospheric loss maximizing received power, and polarization loss. Readers are referred to Betz (2010) for specific details on the aforementioned parameters description. Furthermore, both minimum and maximum GNSS receiver power values increase depending on the satellite elevation angle (e) relative to the receiver antenna. For example, the maximum GPS received power for each frequency varies by approximately ~ 2.3 dBW over elevation angles from 0 to 90 degrees (Betz 2016).

The interface design information for each satellite navigation system (GPS, GLONASS, Galileo, and BeiDou) is formally described in its respective Interface Control Document (ICD). These ICDs contain essential details, constants, parameters, definitions, and procedures concerning the system interface. Each government agency responsible for the respective satellite navigation system maintains and updates its ICD with each new issue. In this study, the information from each ICD was used to calculate the mean of the theoretical minimum power received in units of dBW for each satellite navigation system, frequency band, and satellite block. Additionally, the noise density for a typical in-ground receiver was utilized to convert each value to dB-Hz. The results are summarized in Table 2.

The C/N_0 values of the GNSS observations from the Xiaomi Mi 8 were analyzed considering two factors: (1) the elevation angle of the GNSS satellites, and (2) the theoretical C/N_0 values as proposed in Table 2. Figure 6 shows the relation between the elevation angle of GNSS satellites and their corresponding C/N_0 values for each frequency. The analysis revealed generally low C/N_0 values. The latter should include a degradation in the signal quality in a range of ~ 10 and ~ 15 dB-Hz lower than those recorded by geodetic-grade receivers (Li et al. 2021; Everett et al. 2022;

Table 2 Theoretical minimum and maximum received power levels reported for the different GNSS constellation

GNSS	Band/Block	Minimum Received Power [dB-Hz]	Maximum Received Power [dB-Hz]
GPS [a,b]	L1 C/A	45.5	51
	L1 C	47	51
	L2-II-IIA-IIR	39.5	46
	L2-IIF	42.5	46
	L5	46.1	54
GLONASS [c]	L1	43	48.8
	L2	37	48.8
GALILEO [d]	E1	47	52
	E6	49	54
	E5	49	54
BeiDou [e]	B1I	41	45
	B1C-MEO	45	49
	B1C-IGSO	43	47
	B2A	48	52
	B3I	41	45

[a] GPS-ICD (2022a)

[b] GPS-ICD (2022b)

[c] GLONASS-ICD (2008)

[d] Galileo-ICD (2021)

[e] BeiDou-ICD (2019)

Bramanto et al. 2023). Among the satellites, R14, R15, and R20 displayed the highest C/N_0 values concerning the elevation angle, while GPS, Galileo, and BeiDou experienced the lowest values. It is noteworthy that the highest C/N_0 values for each GNSS constellation did not necessarily occur at the highest elevation angles. Some satellites demonstrated similar C/N_0 magnitudes within the range of 20° to 80° elevation angle (e.g., satellite E25). Consequently, the irregularity of the C/N_0 values in the Xiaomi Mi 8 GNSS observations is attributed to the quality of the antenna (possibly irregular gain) (Pesyna et al. 2014), rather than being influenced by the elevation angle of the satellites (as observed in geodetic-grade antennas) or the antennas environmental conditions.

Figure 7 shows the C/N_0 values as a percentage (%) of the maximum theoretical values obtained from Table 2 for all registered GNSS satellites and frequencies. In general, for both GPS and Galileo, the L1/E1 signal scores were higher compared to L5/E5a. Among the constellations, GLONASS satellites achieved scores close to 100% for some satellites (R02, R11, R12, R24), making it the only constellation to reach this percentage. On the other hand, BeiDou had the lowest percentages in one of its satellites (C26, C32, C37). The mean score for each constellation and frequency is presented in Table 3, with the GLONASS (G1) constellation obtaining the highest score of 88.23%, while Galileo (E5a) displayed the lowest score at 66.40%. These results may be attributed to the design of the GLONASS orbit and the FCC restrictions on the Galileo and BeiDou signals.

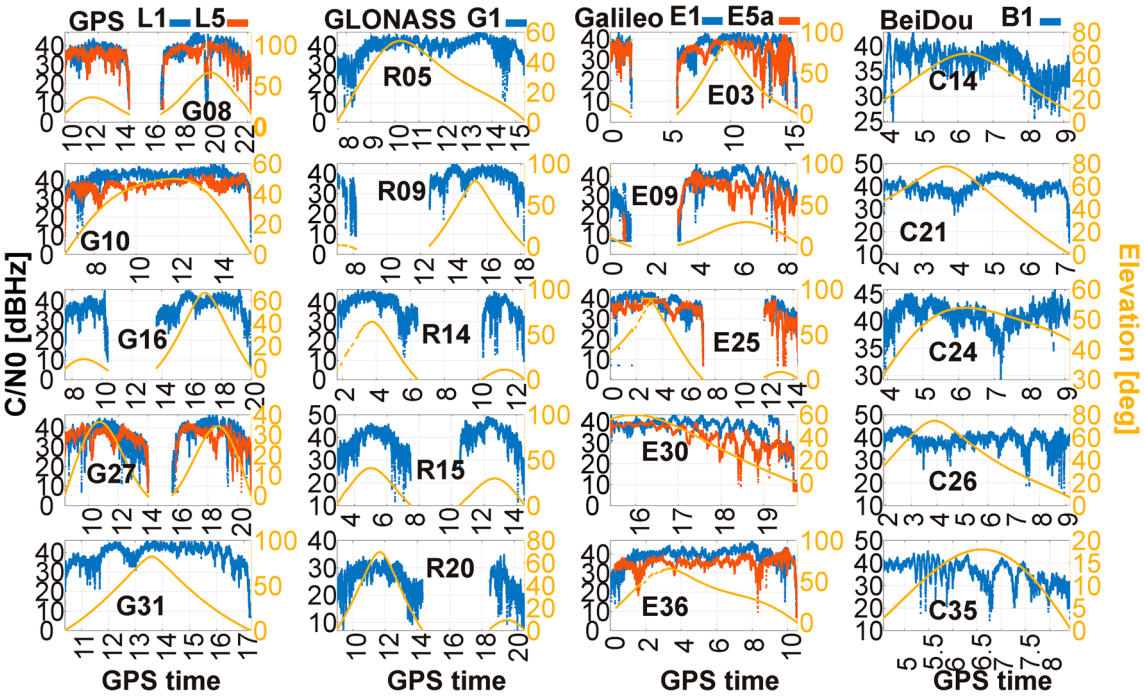

Fig. 6 Relation between the elevation angle of the GNSS satellites and the corresponding values for each frequency and constellation C/N_0 values for each frequency and constellation

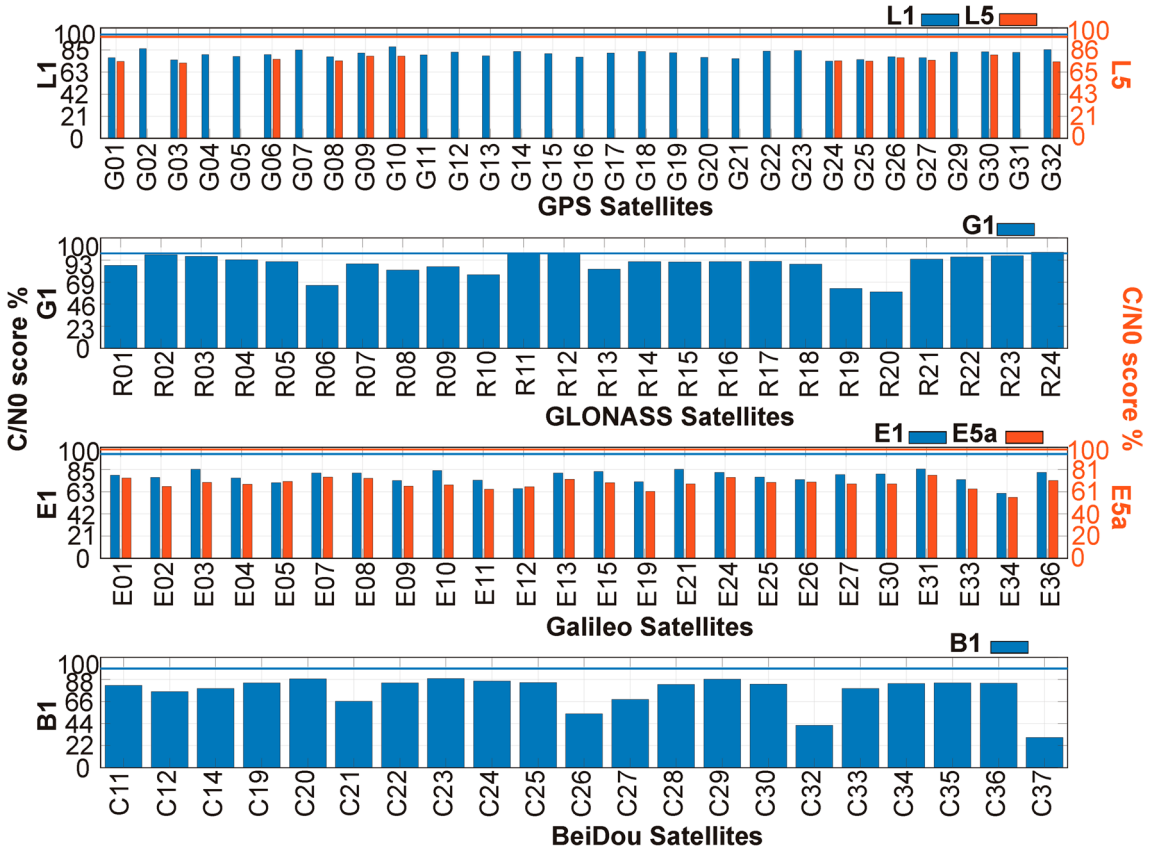

Fig. 7 Percentage of observed C/N_0 values with respect to the theoretical maximum C/N_0 for all satellites and GNSS frequencies recorded by the Xiaomi Mi 8 during the continuous 24-hour measurements. The blue and orange lines represent 100% of the C/N_0 score for single and double frequency, respectively

Table 3 Mean C/N_0 score in percentage (%) for each constellation and frequency

Smartphone	C/N_0 score %					
	GPS		GLONASS	Galileo		BeiDou
	L1	L5	G1	E1	E5a	B1
Xiaomi Mi 8	81.06	77.48	88.23	76.36	66.40	75.04

Pseudorange multipath

The linearly polarized GNSS antenna of the Xiaomi Mi 8 smartphone is susceptible to multipath (Robustelli et al. 2019), which is a significant source of error affecting smartphone positioning accuracy. Multipath is an important indicator of GNSS signal quality (Yun et al. 2022). For that reason, in this study the impact of multipath was evaluated on the GPS and Galileo constellations, that is, the two constellations that emit dual-frequency signals among the registered by the Xiaomi Mi 8. It is noteworthy that this analysis is one of the few studies to examine multipath effects in the pseudorange measurements of a smartphone. Figure 8 illustrates the relation between the elevation angle and multipath values for four GPS and Galileo satellites (the highest elevation). This study found that the L1 and E1 frequencies are affected approximately four and two times more than the L5 and E5a frequencies, respectively. This disparity is attributed to the high chipping rate of L5/E5a (Leclère et al. 2018), making them less susceptible to multipath effects (Circiu et al. 2017).

Figure 8 shows that the elevation angle has minimal impact on the multipath values, which are predominantly influenced by the poor quality of the smartphones GNSS antenna. Conversely, Fig. 9 displays the mean pseudorange multipath values for GPS and Galileo satellites with dual frequency. The mean multipath values for GPS (L1) satellites were consistently around 200 cm, while GPS (L5) exhibited

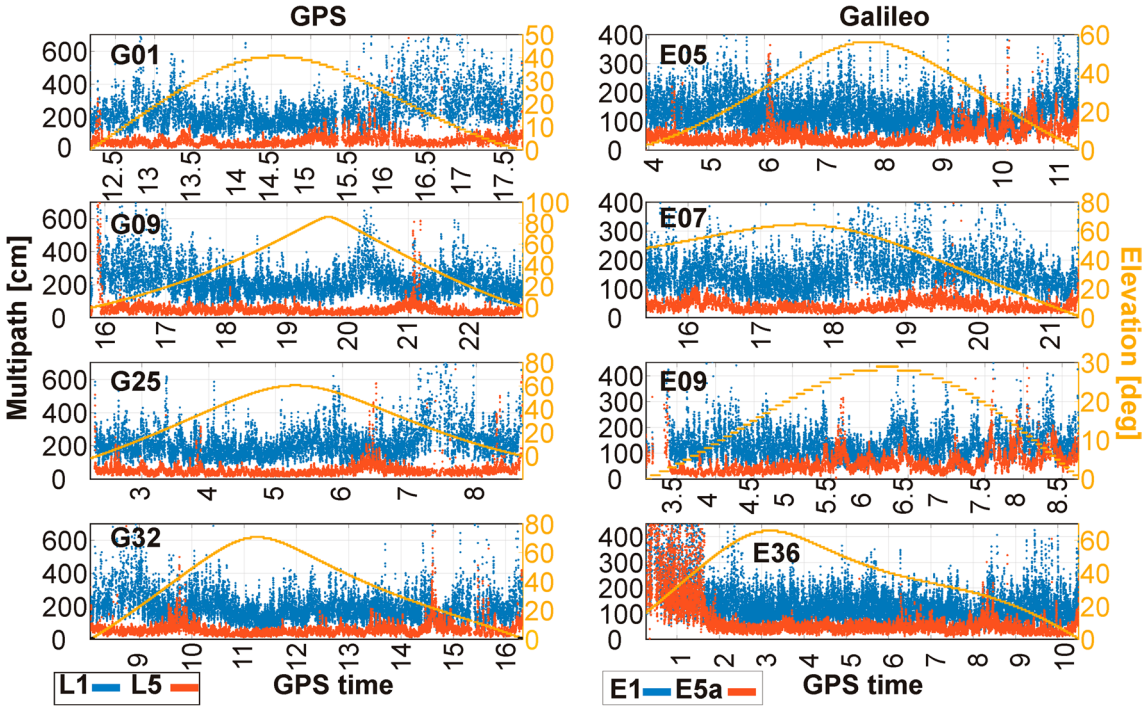

Fig. 8 Relation between multipath and the satellite elevation angle for the dual frequencies of the GPS and Galileo constellations

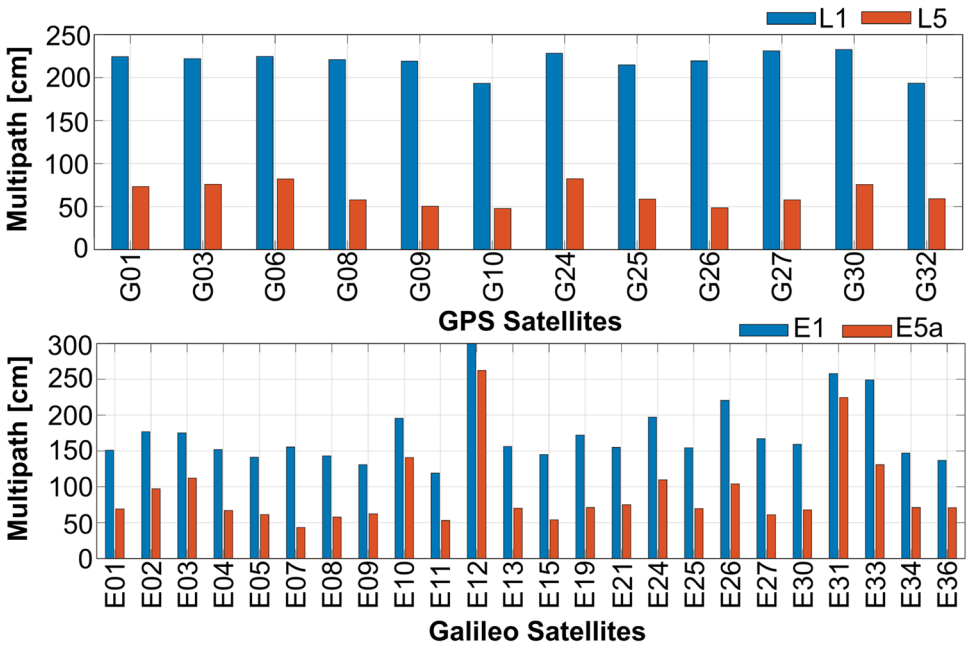

Fig. 9 Average multipath from both dual frequency GPS and Galileo satellites observed by the Xiaomi Mi 8

lower mean values, approximately 80 cm. For Galileo satellites (E1/E5a), the mean multipath values presented a slight difference and were lower than those of GPS. These findings further support the hypothesis that GNSS antenna issues primarily cause multipath errors in smartphones.

Table 4 summarizes the mean multipath error for both the GPS and Galileo constellations. The GPS satellites operating

Table 4 Mean multipath for the GPS and Galileo constellations

Smartphone	Mean multipath [cm]			
	GPS		Galileo	
	L1	L5	E1	E5a
Xiaomi Mi 8	218.7	63.6	168.3	85.3

at L1 and L5 frequencies experienced multipath errors of approximately 2.187 m and 0.636 m, respectively. For the Galileo satellites at E1 and E5a frequencies, the multipath errors were approximately 1.683 m and 0.853 m, respectively. It is important to highlight that the noise level of the GNSS pseudorange observation of the smartphone is high (up to tens of meters) (Paziewski 2020) and is incorporated into the pseudorange multipath. Furthermore, the multipath values for the E1 and E5 signals of the Galileo and L5 GPS satellites presented lower values than those of GPS L1, such as those reported by Circiu et al. (2017). Overall, the mean multipath values for each GPS and Galileo satellite remained below 3 m. It is noteworthy that these values are lower than those reported in other studies (Robustelli et al. 2019).

Kinematic experiment results

Figure 10 illustrates the kinematic solutions of the circular trajectory considering various GNSS combinations, including G, G + E, G + R + E + C, and G + R + C. To assess the kinematic performance of the Xiaomi Mi 8, the root mean square (RMS) was utilized as an indicator of precision. The RMS was computed based on the difference between the reference distance (19 cm) and the distances calculated using the East (E) and North (N) coordinates. The smoothest trajectory was achieved with the G + E combination, which exhibited an RMS of 1.4 cm. Comparatively, the other combinations yielded similar RMS values, with differences of less than 0.9 cm.

By leveraging multi-GNSS and multi-frequency observations from a Xiaomi Mi 8 smartphone, kinematic measurements can attain precisions of less than 2 cm. The experiment was conducted in a location with unobstructed sky visibility, which played a significant role in achieving accurate results. Additionally, establishing a baseline of less than 8 km further contributed to achieving horizontal component accuracies comparable to those of low-cost GNSS receivers. However, it should be noted that due to the lack of a vertical reference in the ensemble, the evaluation was focused solely on the horizontal component. Nonetheless, the study findings highlight the potential of using a Xiaomi Mi 8 smartphone with multi-GNSS and multi-frequency capabilities for precise kinematic measurements in practical engineering applications, such as structural monitoring.

GNSS Positioning performance of the Xiaomi Mi 8

The experiment was conducted on the roof of the Faculty of Earth and Space Sciences at the Autonomous University of Sinaloa in Mexico. To assess the precise three-dimensional positioning performance of the Xiaomi Mi 8, a baseline of approximately 10 m was set up. The reference station comprised a low-cost Mosaic X5 receiver and a LEIAS AS10 geodetic antenna. The Xiaomi Mi 8 was configured as a rover

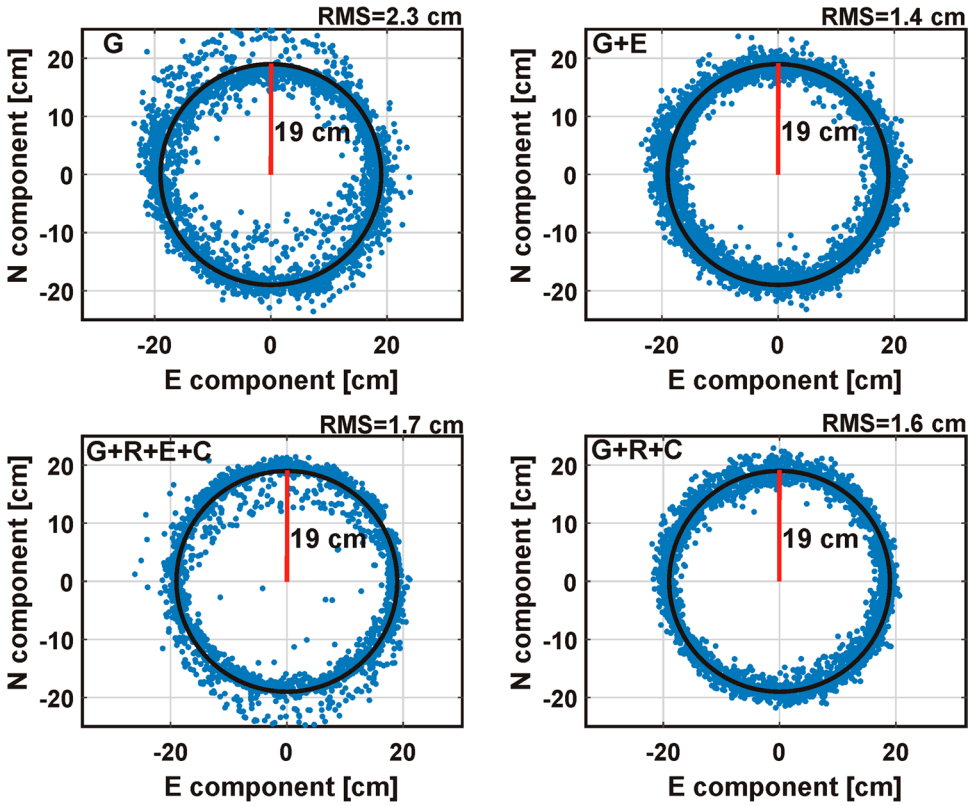

Fig. 10 Circular trajectory tracking of kinematic results obtained from various GNSS combinations. The blue dots represent the kinematic solutions of the Xiaomi Mi 8, and the black circle represent the reference circular movement

and set on a vertically forced centering monument with the help of a fixed support on a tribrach. Using geodetic order equipment and the relative static method, precise coordinates for the forced centering monument were determined. In contrast, processing in PPP mode was negligible since the precision achieved by the latter using smartphone observations is on the order of meters (Robustelli et al. 2019). Also, an ENU (East-North-Up) topocentric coordinate system with origin at the reference station was established. The Xiaomi Mi 8 antenna was oriented to the North, as illustrated in Fig. 11.

To achieve precise centering at ~1 cm accuracy, the Antenna Reference Point (ARP) located on the top of the Xiaomi Mi 8 was taken into consideration (refer to Fig. 11). The distance between the ARP and CRP (Centering Reference Point) was measured, and using the phase center location of the antenna reported by Netthonglang et al. (2019), displacements of the general phase center were estimated and presented in Table 5. As a result, the coordinates obtained by the Xiaomi Mi 8 were referenced to the CRP, which is the same reference point as the known coordinates of the forced centering monument. This was done to evaluate the positioning performance of the Xiaomi Mi 8 by comparing its reference coordinates with those estimated by the smartphone.

During the experiment, a total of 11 GPS satellites, 10 GLONASS satellites, 5 Galileo satellites, and 6 BeiDou satellites were visible. Observations were collected at a sampling frequency of 1 s using the Geo++RINEX Logger app, and the data was gathered for a duration of one hour. To ensure accuracy, Wi-Fi and Bluetooth were disabled during data collection. The GNSS observations from the low-cost reference receiver and the Xiaomi Mi 8 were saved in RINEX 3.04 format to be later processed in relative static mode using the RTKLIB software (Takasu and Yasuda 2009; Everett et al. 2022).

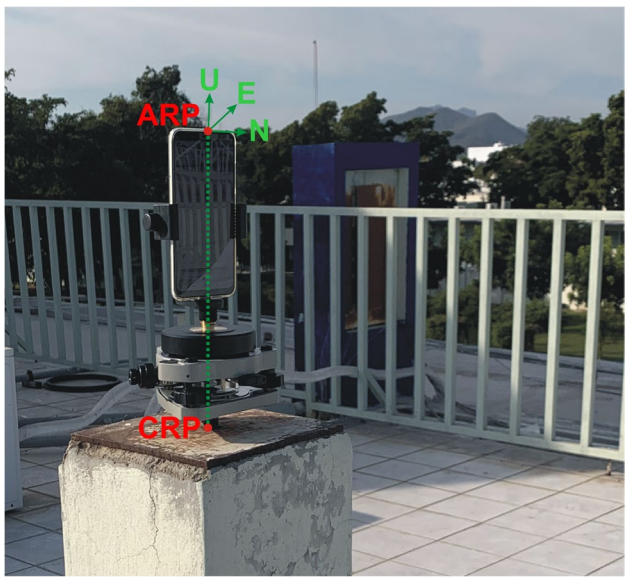

Fig. 11 Xiaomi Mi 8 vertically centered and leveled on a force-centered monument. Setting of ENU coordinates and antenna orientation

Table 5 Offset of Xiaomi Mi 8 antenna phase center with respect to the CRP

North (cm)	East (cm)	Up (cm)
2.8	1	28

Processing strategies

The Xiaomi Mi 8 GNSS observations were processed using the open-source software RTKLIB demo5 b34g (Takasu and Yasuda 2009; Everett et al. 2022) with processing strategies outlined in Table 6. To evaluate multi-GNSS positioning performance, 8 GNSS combinations were established: G, E, G + R + E + C, G + E, G + R + E, R + E, R + E + C and E + C. Previous studies have evaluated relative positioning by means of geodetic-grade GNSS receivers and smartphones (Geng and Li 2019; Uradziński and Bakuła 2020) and smartphones only (Paziewski et al. 2021). These studies demonstrated centimeter-level differences between the estimated solutions and the reference values. In this study, we established a short baseline comprising a Xiaomi Mi 8 smartphone and a low-cost GNSS receiver with a geodetic-grade antenna.

Table 6 Processing strategies for the RTKLIB software demo5b34g

Items	Strategy
Mode	static
Frequency observed	GPS L1/L5, GLONASS L1, Galileo E1/E5a, BeiDou B1
Observation type	Code and Carrier Phase
Filter type	Combined
Sampling rate	1 s
Cutoff elevation angle	12°
C/N_0 Mask	20 dBHz
GNSS orbit and clock	Broadcast ephemeris
Tropospheric delay	Saastamoinen model
Ionospheric delay	Broadcast ephemeris
Stochastic model	Carrier-phase noise (a0,b0): 0.003 m Code-carrier error ratio: 300:1
Ambiguity resolution mode	Fix and hold
Antex file	ngs14.atx
Output coordinates	E/N/U

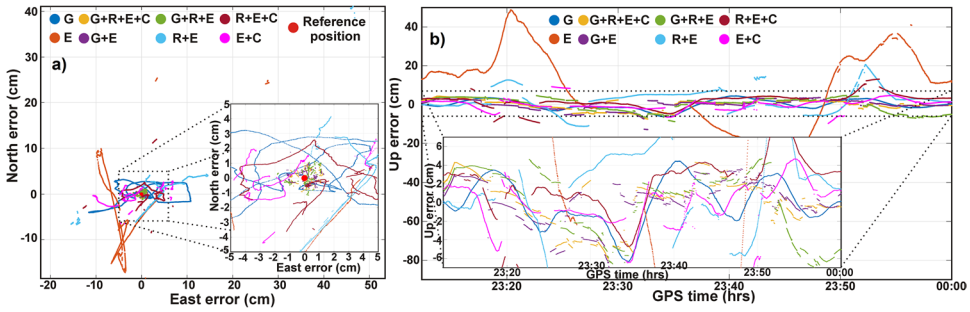

Fig. 12 Relative static positioning errors for GNSS combinations. **a** horizontal error; **b** vertical error

Static experiment results

Figure 12 illustrates the relative static positioning errors of the smartphone for each GNSS combination. Significant discrepancies were observed in specific combinations, including G, E, E + C and R + E + C, which exhibited the most pronounced discrepancies in both the horizontal and vertical components. In addition, the positioning performance of the Xiaomi Mi 8 was evaluated using precision indicators such as the mean ($\bar{x}$), standard deviation (σ) and root mean square error (RMSE). Table 7 presents these precision indicators for each GNSS combination. Among the combinations tested, G + R + E + C exhibited the best precision, with RMS values of 0.7 cm, 1.2 cm, and 4.2 cm for the East, North, and Up components, respectively. Notably, combinations involving both GPS and Galileo showed similar accuracies, indicating that achieving high precision and fixing ambiguities in three-dimensional positioning with a smartphone requires using both GPS and Galileo constellations simultaneously. Conversely, the combination R + E resulted in the lowest precision, with RMS values of 27.6 cm, 14.9 cm, and 45.1 cm for the East, North, and Up components, respectively. Furthermore, the performance of using only GPS or Galileo constellations was poor in achieving fixed ambiguity percentages. Therefore, it is not recommended to rely solely on isolated GPS or Galileo constellations for relative positioning using a Xiaomi Mi 8 smartphone.

GPS and Galileo are the most desirable constellations to obtain reliable static positioning accuracy with GNSS measurements from a Xiaomi Mi 8 smartphone due to the availability of dual-frequency transmissions (Magalhães et al. 2021; Purfürst 2022; Yun et al. 2022), such as those achieved in this study. In contrast, GLONASS and BeiDou are less recommended due to their limited capability to track dual frequencies that represents a lower precision as reported in Table 7 where these constellations only in combination with other constellations (GPS or Galileo) achieved fixed ambiguity solutions.

Conclusions and future work

This study evaluates the GNSS signal quality recorded from a Xiaomi Mi 8 smartphone and proposes a signal evaluation strategy based on theoretical C/N_0 values. The performance of kinematic and static positioning is also analyzed. The results reveal that the smartphones GNSS observations have lower quality compared to theoretical reference values, particularly for GPS, Galileo, and BeiDou, which are not affected by the elevation angle.

Table 7 Statistical summary of static relative positioning errors

GNSS Combinations	# Total satellites	Fixing rate (%)	Position error								
			East (cm)			North (cm)			Up (cm)		
			$\bar{x}$	σ	RMS	$\bar{x}$	σ	RMS	$\bar{x}$	σ	RMS
G	11	-	4.9	5.3	7.3	7.3	1.8	7.5	13.2	2.4	13.4
E	5	21.8	1.5	14.2	14.3	5	16.5	17.2	5	39.3	39.8
G + R + E + C	32	100%	-0.3	0.65	0.7	-1.1	0.45	1.2	-3.3	2.6	4.2
G + E	16	99.3	-0.2	0.7	0.7	-1.1	0.4	1.1	-4.1	2.5	4.8
G + R + E	26	99.7	-0.4	0.79	0.9	-1.1	0.54	1.2	-2.9	3.7	4.7
R + E	15	39.1	5.7	27	27.6	-6.5	13.4	14.9	40.2	20.4	45.1
R + E + C	21	15.6	7.9	22.3	23.7	-2.8	9.2	9.6	21.2	14.2	25.5
E + C	11	48.5	3.6	15.9	16.35	0.2	9.4	9.4	7.7	16.6	18.3

The C/N_0 values of GLONASS satellites are the only ones that present a high correlation with the satellite elevation angle. The average C/N_0 score for GPS (L1/L5), GLONASS (G1), Galileo (E1/E5a), and BeiDou (B1) is reported as 81.06/77.48%, 88.23%, 76.36/66.10%, and 75.04%, respectively, with an overall average 18% below theoretical reference values, mainly attributed to the bad quality smartphones GNSS antenna. However, this does not impede precise positioning. Moreover, the study found that the L1 and E1 frequencies were particularly susceptible to multipath errors, with mean values of 218.7 cm and 168.3 cm, respectively. In contrast, the L5 and E5a frequencies exhibited lower multipath errors, with values less than 86 cm. The main cause of the multipath generation on the Xiaomi Mi 8 smartphone is attributed to the linear polarization of the GNSS antenna. This study did not find a direct correlation between the occurrence of multipath errors and the elevation angle of the satellites.

Using smartphone multi-frequency and multi-constellation observations enables sub-centimeter and centimeter-level accuracies in static and kinematic positioning, respectively. In the kinematic experiment, the Xiaomi Mi 8 achieves an RMS error of 1.4 cm in the horizontal component while following a circular trajectory. For the G + R + E + C combination, static positioning results show RMS errors of 0.7 cm, 1.2 cm, and 4.2 cm in the East, North, and Up components, respectively.

The achieved results demonstrate the Xiaomi Mi 8 potential as a valuable tool in engineering sciences. Therefore, our future work will focus on utilizing the latest GNSS chipsets capable of tracking dual-frequency signals for structural health monitoring in bridge applications.

Acknowledgements The authors express their gratitude to the Autonomous University of Sinaloa for their support in conducting this study. Special thanks are extended to the National Council of Humanities, Sciences, and Technologies (CONAHCyT) in Mexico for granting a scholarship to accomplish this study. However, it should be noted that the results, observations, and conclusions presented in this paper are solely those of the authors and do not necessarily reflect the views of the sponsoring organizations.

Author contributions J.R.V.O: Conceptualization, Methodology, Software, Data curation, Writing - Original draft preparation, Visualization, Validation. C.A.M.F: Visualization, Investigation, Supervision, Writing- Original draft preparation. A.M.M: Writing- Reviewing and Editing. L.R.S: Writing- Reviewing and Editing. G.E.V.B: Reviewing. J.R.G.C: Reviewing. All authors read and approved the final manuscript.

Funding This research work was funded by to the National Council of Humanities, Sciences, and Technologies (CONAHCyT) in Mexico by the grant # 859589.

Data availability The datasets analyzed during the current study is available in the data repository of Zenodo (https://doi.org/10.5281/zenodo.8206887).

Code availability The Open-Source Program Package for RTK-GPS used to process the GNSS observations retrieved by the smartphone was developed by Tomoji Takasu and is available under the GNU General Public License. The program package can be accessed and downloaded from the website: (https://rtklib.com/).

Declarations

Competing interests The authors declare no competing interests.

References

Aggrey J, Bisnath S, Naciri N, Shinghal G, Yang S (2020) Multi-GNSS precise point positioning with next-generation smartphone measurements. J Spat Sci 65(1):79–98. https://doi.org/10.1080/14498596.2019.1664944

Bahadur B (2022) A study on the real-time code-based GNSS positioning with android smartphones. Measurement 194:111078. https://doi.org/10.1016/j.measurement.2022.111078

Bakuła M, Uradziński M, Krasuski K (2020) Network Code DGNSS positioning for faster L1–L5 GPS ambiguity initialization. Sensors 20(19):5671. https://doi.org/10.3390/s20195671

Bakuła M, Uradziński M, Krasuski K (2022) Performance of DGPS smartphone positioning with the use of P(L1) vs. P(L5) pseudorange measurements. Remote Sens 14(4):929. https://doi.org/10.3390/rs14040929

BeiDou-ICD (2019) BeiDou Interface Control Document (BDS-SIS-ICD-B1I-3.0 for B1). China Satellite Navigation Office. http://en.beidou.gov.cn/SYSTEMS/ICD/201902/P020190227702348791891.pdf. Accessed May 2023

Betz JW (2010) Link Budgets. 5th annual meeting of the International Committee on GNSS (ICG), Turin, Italy, pp 1–15. Accessed April 2023

Betz JW (2016) Engineering satellite-based navigation and timing: global navigaton satellite systems, signals, and receivers. IEEE Press; Wiley, Piscataway (Accessed April 2023)

Bramanto B, Gumilar I, Kuswanti IAN (2023) Assessment of GNSS observations and positioning performance from non-flagship android smartphones. J Appl Geod 0(0). https://doi.org/10.1515/jag-2023-0033

Chen B, Gao C, Liu Y, Sun P (2019) Real-time precise point positioning with a Xiaomi MI 8 Android Smartphone. Sensors 19(12):2835. https://doi.org/10.3390/s19122835

Cheng S, Wang F, Li G, Geng J (2023) Single-frequency multi-GNSS PPP-RTK for smartphone rapid centimeter-level positioning. IEEE Sens J 23(18):21553–21561. https://doi.org/10.1109/JSEN.2023.3301658

Circiu M-S, Meurer M, Felux M, Gerbeth D, Thölert S, Vergara M, Enneking C, Sgammini M, Pullen S, Antreich F (2017) Evaluation of GPS L5 and Galileo E1 and E5a performance for future multifrequency and multiconstellation GBAS: evaluation of GPS L5 and Galileo E1 and E5a. Navigation 64(1):149–163. https://doi.org/10.1002/navi.181

Dabove P, Di Pietra V, Piras M (2020) GNSS positioning using mobile devices with the android operating system. ISPRS Int J Geo-Inf 9(4):220. https://doi.org/10.3390/ijgi9040220

Everett T, Taylor T, Lee D-K, Akos DM (2022) Optimizing the Use of RTKLIB for smartphone-based GNSS measurements. Sensors 22(10):3825. https://doi.org/10.3390/s22103825

Federal Communications Commission F (2023) Code of Federal Regulations, Title 47. Government Printing Office. https://bookstore.gpo.gov/catalog/cfr-title-47-telecommunication. Accessed March 2023

Fortunato M, Ravanelli M, Mazzoni A (2019) Real-time geophysical applications with Android GNSS Raw measurements. Remote Sens 11(18):2113. https://doi.org/10.3390/rs11182113

Galileo -ICD (2021) Galileo interface control document (Galileo-OS-SIS-ICD-2.0 for E1, E6 and E5). European GNSS (Galileo) Open Service. https://www.gsc-europa.eu/sites/default/files/sites/all/files/Galileo_OS_SIS_ICD_v2.0.pdf. Accessed May 2023

Gao R, Xu L, Zhang B, Liu T (2021) Raw GNSS observations from Android smartphones: characteristics and short-baseline RTK positioning performance. Meas Sci Technol 32(8):084012. https://doi.org/10.1088/1361-6501/abe56e

Geng J, Li G (2019) On the feasibility of resolving Android GNSS carrier-phase ambiguities. J Geod 93(12):2621–2635. https://doi.org/10.1007/s00190-019-01323-0

GLONASS-ICD (2008) GLONASS Interface Control Document (L1 and L2). Russian Institute of Space Device Engineering. http://gauss.gge.unb.ca/GLONASS.ICD.pdf. Accessed May 2023

GPS-ICD (2022a) GPS Interface Control Document (IS-GPS-200 for L1 and L2). U.S. National Coordination Office for Space-Based Positioning, Navigation, and Timing. https://www.gps.gov/technical/icwg/IS-GPS-200N.pdf. Accessed May 2023

GPS-ICD (2022b) GPS Interface Control Document (IS-GPS-705 for L5). U.S. National Coordination Office for Space-Based Positioning, Navigation, and Timing. https://www.gps.gov/technical/icwg/IS-GPS-705J.pdf. Accessed May 2023

Guo L, Wang F, Sang J, Lin X, Gong X, Zhang W (2020) Characteristics analysis of raw multi-GNSS measurement from Xiaomi Mi 8 and positioning performance improvement with L5/E5 frequency in an urban environment. Remote Sens 12(4):744. https://doi.org/10.3390/rs12040744

Langley RB (1997) GPS Receiver System Noise. In: Innovation. GPS World. University of New Brunswick, Canada, pp 40–45. http://gauss2.gge.unb.ca/papers.pdf/gpsworld.june97.pdf. Accessed Apr 2023

Leclère J, Landry R Jr, Botteron C (2018) Comparison of L1 and L5 bands GNSS signals acquisition. Sensors 18(9):2779. https://doi.org/10.3390/s18092779

Li G, Geng J (2019) Characteristics of raw multi-GNSS measurement error from Google Android smart devices. GPS Solut 23(3):90. https://doi.org/10.1007/s10291-019-0885-4

Li G, Geng J, Chu B (2023) High-precision velocity determination using mass-market Android GNSS measurements in the case of anomalous clock variations. GPS Solut 27(3):98. https://doi.org/10.1007/s10291-023-01440-6

Li M, Lei Z, Li W, Jiang K, Huang T, Zheng J, Zhao Q (2021) Performance evaluation of single-frequency Precise point positioning and its use in the android smartphone. Remote Sens 13(23):4894. https://doi.org/10.3390/rs13234894

Liu Q, Gao C, Peng Z, Zhang R, Shang R (2021) Smartphone positioning and accuracy analysis based on real-time regional ionospheric correction model. Sensors 21(11):3879. https://doi.org/10.3390/s21113879

Liu W, Shi X, Zhu F, Tao X, Wang F (2019) Quality analysis of multi-GNSS raw observations and a velocity-aided positioning approach based on smartphones. Adv Space Res 63(8):2358–2377. https://doi.org/10.1016/j.asr.2019.01.004

Magalhães A, Bastos L, Maia D, Gonçalves JA (2021) Relative positioning in remote areas using a GNSS dual frequency smartphone. Sensors 21(24):8354. https://doi.org/10.3390/s21248354

Netthonglang C, Thongtan T, Satirapod C (2019) GNSS precise positioning determinations using smartphones. In: 2019 IEEE Asia Pacific Conference on Circuits and Systems (APCCAS). IEEE, Bangkok, Thailand, pp 401–404

Odolinski R, Teunissen PJG (2019) An assessment of smartphone and low-cost multi-GNSS single-frequency RTK positioning for low, medium and high ionospheric disturbance periods. J Geod 93(5):701–722. https://doi.org/10.1007/s00190-018-1192-5

Paziewski J (2020) Recent advances and perspectives for positioning and applications with smartphone GNSS observations. Meas Sci Technol 31(9):091001. https://doi.org/10.1088/1361-6501/ab8a7d

Paziewski J, Fortunato M, Mazzoni A, Odolinski R (2021) An analysis of multi-GNSS observations tracked by recent android smartphones and smartphone-only relative positioning results. Measurement 175:109162. https://doi.org/10.1016/j.measurement.2021.109162

Paziewski J, Sieradzki R, Baryla R (2019) Signal characterization and assessment of code GNSS positioning with low-power consumption smartphones. GPS Solut 23(4):98. https://doi.org/10.1007/s10291-019-0892-5

Pepe M, Costantino D, Vozza G, Alfio VS (2021) Comparison of two approaches to GNSS positioning using code pseudoranges generated by smartphone device. Appl Sci 11(11):4787. https://doi.org/10.3390/app11114787

Pesyna KM, Heath RW Jr, Humphreys TE (2014) Centimeter positioning with a smartphone-quality GNSS Antenna. Proceedings of the 27th International Technical Meeting of the Satellite Division of The Institute of Navigation (ION GNSS + 2014), Tampa, Florida, pp 1568–1577

Purfürst T (2022) Evaluation of static autonomous GNSS positioning accuracy using Single-, Dual-, and Tri-frequency smartphones in forest canopy environments. Sensors 22(3):1289. https://doi.org/10.3390/s22031289

Realini E, Caldera S, Pertusini L, Sampietro D (2017) Precise GNSS positioning using Smart devices. Sensors 17(10):2434. https://doi.org/10.3390/s17102434

Robustelli U, Baiocchi V, Pugliano G (2019) Assessment of dual frequency GNSS observations from a Xiaomi Mi 8 android smartphone and positioning performance analysis. Electronics 8(1):91. https://doi.org/10.3390/electronics8010091

Robustelli U, Paziewski J, Pugliano G (2021) Observation quality assessment and performance of GNSS standalone positioning with code pseudoranges of dual-frequency android smartphones. Sensors 21(6):2125. https://doi.org/10.3390/s21062125

Shinghal G, Bisnath S (2021) Conditioning and PPP processing of smartphone GNSS measurements in realistic environments. Satell Navig 2(1):10. https://doi.org/10.1186/s43020-021-00042-2

Specht C, Szot T, Dąbrowski P, Specht M (2020) Testing GNSS receiver accuracy in Samsung Galaxy series mobile phones at a sports stadium. Meas Sci Technol 31(6):064006. https://doi.org/10.1088/1361-6501/ab75b2

Takasu T, Yasuda A (2009) Development of the low-cost RTK-GPS receiver with an open source program package RTKLIB. In: International Symposium on GPS/GNSS. Inside GNSS, Jeju, Korea, pp 1–6

Tomaštík J, Chudá J, Tunák D, Chudý F, Kardoš M (2021) Advances in smartphone positioning in forests: dual-frequency receivers and raw GNSS data. For Int J for Res 94(2):292–310. https://doi.org/10.1093/forestry/cpaa032

Tomaštík J, Varga M (2021) Practical applicability of processing static, short-observation-time raw GNSS measurements provided by a smartphone under tree vegetation. Measurement 178:109397. https://doi.org/10.1016/j.measurement.2021.109397

Uradziński M, Bakuła M (2020) Assessment of static positioning accuracy using low-cost smartphone GPS devices for geodetic survey points' determination and monitoring. Appl Sci 10(15):5308. https://doi.org/10.3390/app10155308

Vaclavovic P, Dousa J (2015) G-Nut/Anubis: open-source tool for multi-GNSS data monitoring with a multipath detection for new signals, frequencies and constellations. In: Rizos C, Willis P (eds) IAG 150 years. Springer International Publishing, Cham, pp 775–782

Wang L, Li Z, Wang N, Wang Z (2021) Real-time GNSS precise point positioning for low-cost smart devices. GPS Solut 25(2):69. https://doi.org/10.1007/s10291-021-01106-1

Wanninger L, Heßelbarth A (2020) GNSS code and carrier phase observations of a Huawei P30 smartphone: quality assessment and centimeter-accurate positioning. GPS Solut 24(2):64. https://doi.org/10.1007/s10291-020-00978-z

Wen Q, Geng J, Li G, Guo J (2020) Precise point positioning with ambiguity resolution using an external survey-grade antenna enhanced dual-frequency android GNSS data. Measurement 157:107634. https://doi.org/10.1016/j.measurement.2020.107634

Wu Q, Sun M, Zhou C, Zhang P (2019) Precise point positioning using dual-frequency GNSS observations on Smartphone. Sensors 19(9):2189. https://doi.org/10.3390/s19092189

Yi D, Bisnath S, Naciri N, Vana S (2021) Effects of ionospheric constraints in precise point positioning processing of geodetic, low-cost and smartphone GNSS measurements. Measurement 183:109887. https://doi.org/10.1016/j.measurement.2021.109887

Yi D, Yang S, Bisnath S (2022) Native Smartphone single- and dual-frequency GNSS-PPP/IMU solution in real-world driving scenarios. Remote Sens 14(14):3286. https://doi.org/10.3390/rs14143286

Yong CZ, Harima K, Rubinov E, McClusky S, Odolinski R (2022) Instantaneous best integer equivariant position estimation using Google Pixel 4 smartphones for single- and Dual-Frequency, Multi-GNSS short-baseline RTK. Sensors 22(10):3772. https://doi.org/10.3390/s22103772

Yong CZ, Odolinski R, Zaminpardaz S, Moore M, Rubinov E, Er J, Denham M (2021) Instantaneous, Dual-Frequency, Multi-GNSS Precise RTK Positioning using Google Pixel 4 and Samsung Galaxy S20 smartphones for Zero and Short Baselines. Sensors 21(24):8318. https://doi.org/10.3390/s21248318

Yun J, Lim C, Park B (2022) Inherent limitations of Smartphone GNSS Positioning and effective methods to increase the accuracy utilizing dual-frequency measurements. Sensors 22(24):9879. https://doi.org/10.3390/s22249879

Zangenehnejad F, Gao Y (2021) GNSS smartphones positioning: advances, challenges, opportunities, and future perspectives. Satell Navig 2(1):24. https://doi.org/10.1186/s43020-021-00054-y

Zeng S, Kuang C, Yu W (2022) Evaluation of real-time kinematic positioning and deformation monitoring using Xiaomi Mi 8 Smartphone. Appl Sci 12(1):435. https://doi.org/10.3390/app12010435

Zhang X, Tao X, Zhu F, Shi X, Wang F (2018) Quality assessment of GNSS observations from an android N smartphone and positioning performance analysis using time-differenced filtering approach. GPS Solut 22(3):70. https://doi.org/10.1007/s10291-018-0736-8

Zhu H, Xia L, Wu D, Xia J, Li Q (2020) Study on Multi-GNSS precise point positioning performance with adverse effects of satellite signals on android smartphone. Sensors 20(22):6447. https://doi.org/10.3390/s20226447